

Structural characterization of a new fluorophosphotellurite glass system

Renato Grigolon Capelo^{1#}, Josef Maximilian Gerdes^{2#}, Ulrich Rehfuß^{3#}, Lais Dantas Silva⁵, Michael Ryan Hansen^{2*}, Leo van Wüllen^{3*}, Hellmut Eckert^{2,4*}, Danilo Manzani^{1*}

¹*São Carlos Institute of Chemistry – IQSC, University of São Paulo – USP, São Carlos, SP, Brazil*

²*Institut of Physical Chemistry, WWU Münster, Germany*

³*Physics Institute, University of Augsburg, Germany*

⁴*São Carlos Institute of Physics – IFSC, University of São Paulo – USP, São Carlos, SP, Brazil*

⁵*Center of Research, Technology, and Education in Vitreous Materials (CeRTEV), Department of Materials Engineering (DEMa), Federal University of São Carlos (UFSCar), 13565-905, São Carlos, SP, Brazil.*

Equally contributing authors

Supplemental Materials

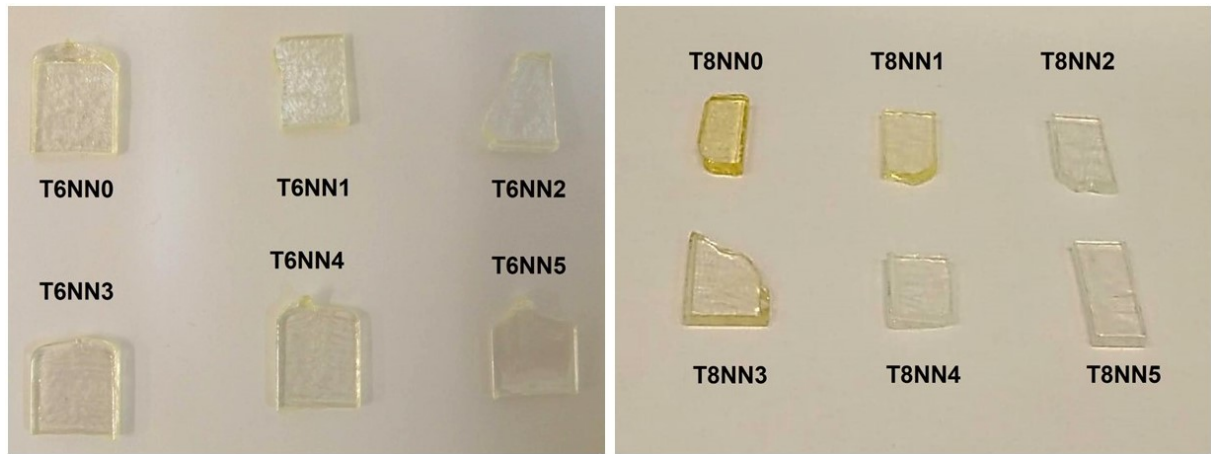


Figure S1. Photographs of the T6 and T8 set of glass samples.

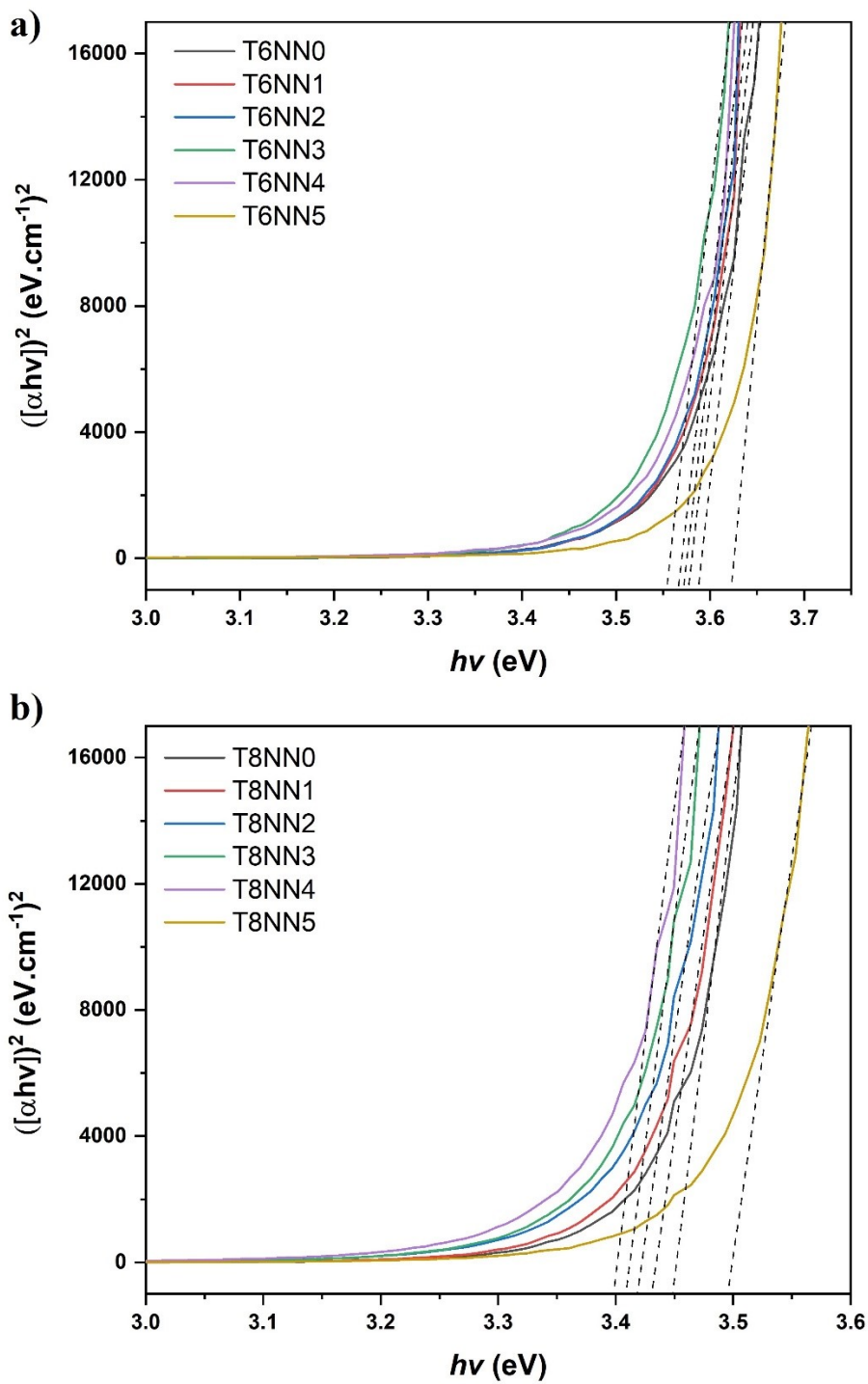


Figure S2. Curves $[\alpha(hv)]^2$ vs. $h\nu$ obtained from the absorption spectra of (a) T6, and (b) T8 set of glass samples.

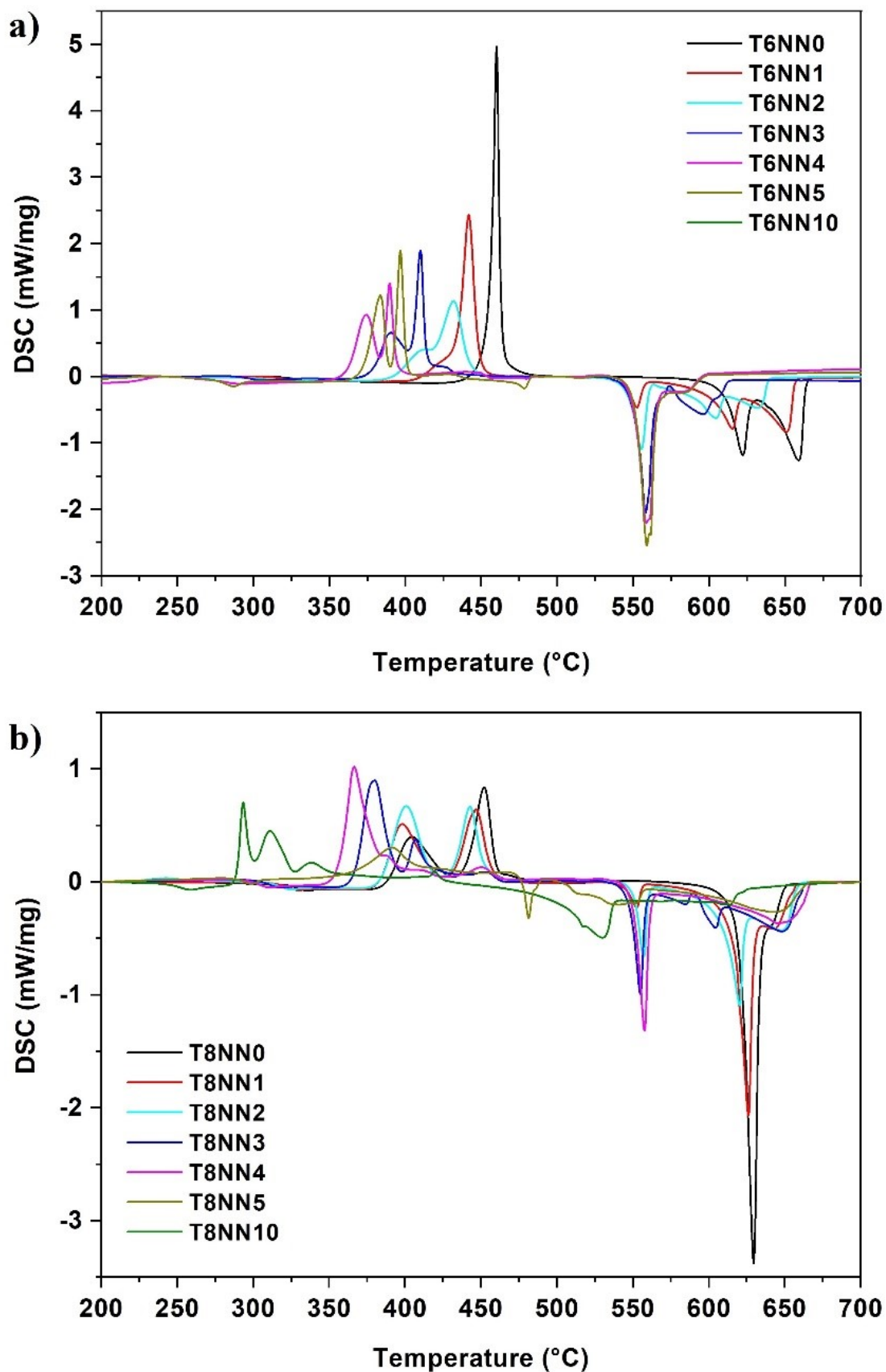


Figure S3. DSC curves for (a) series T6; and (b) series T8 of fluorophosphotellurite powder samples.

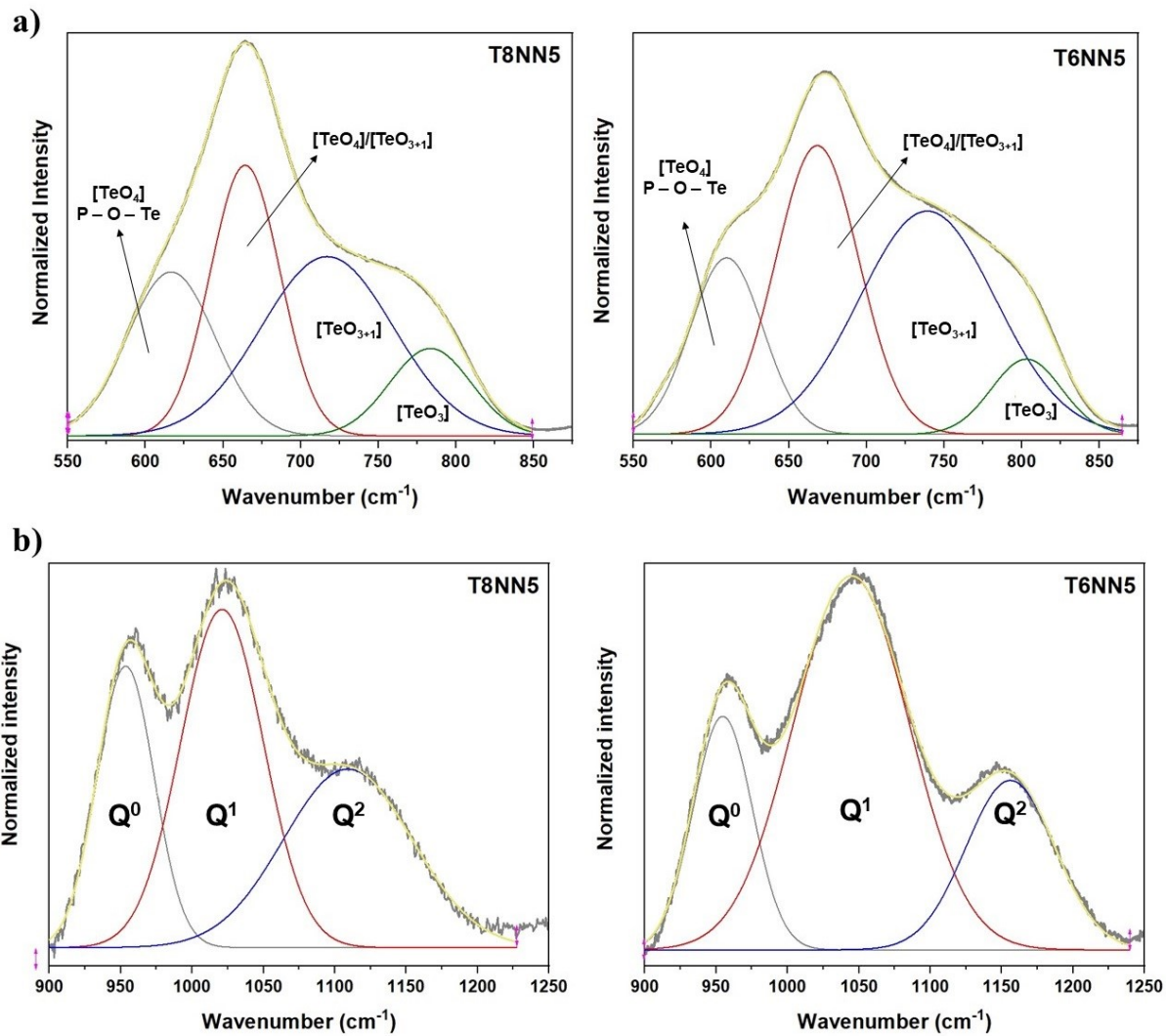


Figure S4. Representative Raman deconvoluted bands between (a) 550 to 900 cm⁻¹ (tellurite bands), and (b) 900 to 1250 cm⁻¹ (phosphate bands) for the T8NN5 and T6NN5 samples.

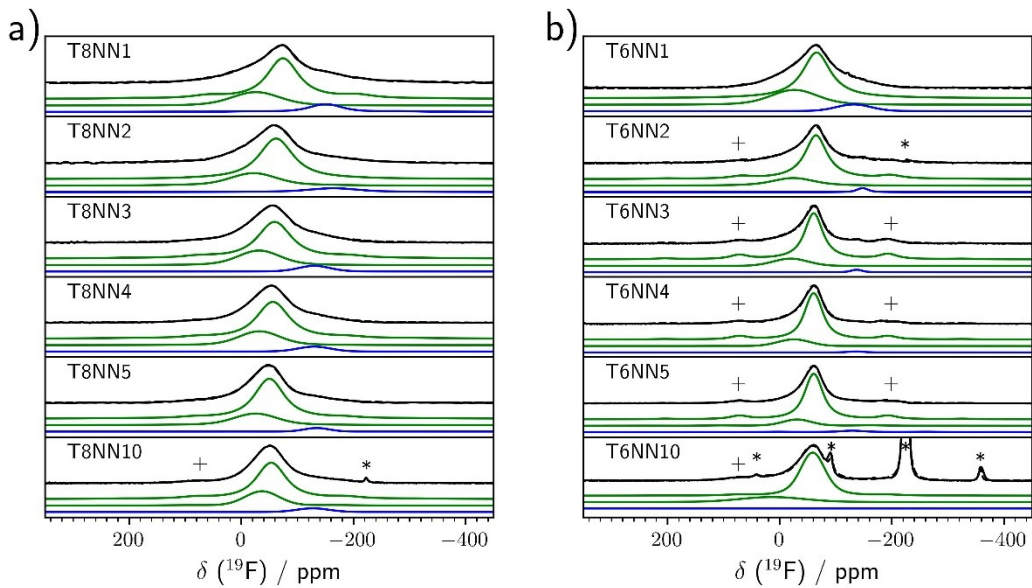


Figure S5. ^{19}F MAS NMR spectra of the samples under study, recorded with a rotor-synchronized Hahn-echo sequence at a rotation frequency of 25 kHz. Experimental spectra are shown on top with each fit component from tentative deconvolutions stacked below in green and blue. Visible spinning side bands are marked with a + symbol, impurities of NaF with their respective spinning sidebands are marked with asterisks.

Table S3. Isotropic chemical shifts and fractional area in percent of the integral as obtained from the tentative fits to the ^{19}F MAS NMR spectra to three distinct components.

Sample	Component 1		Component 2		Component 3	
	δ / ppm	Area / %	δ / ppm	Area / %	δ / ppm	Area / %
T6NN1	-25.1	27	-65.0	65	-131.2	8
T6NN2	-23.5	19	-63.9	79	-147	2
T6NN3	-18.7	14	-59.8	84	-136.3	2
T6NN4	-24.6	14	-59.7	85	-135.1	1
T6NN5	-30.3	14	-59.9	82	-129	4
T6NN10	14.6	21	-58.1	79		
T8NN1	-25.2	23	-73.4	66	-149.7	11
T8NN2	-21.0	24	-61.2	67	-163	9
T8NN3	-30.8	24	-58.4	69	-129.3	7
T8NN4	-31.4	24	-55.5	69	-129.1	7
T8NN5	-24.5	24	-49.2	72	-133.7	4
T8NN10	-36.1	24	-52.5	71	-126.8	5

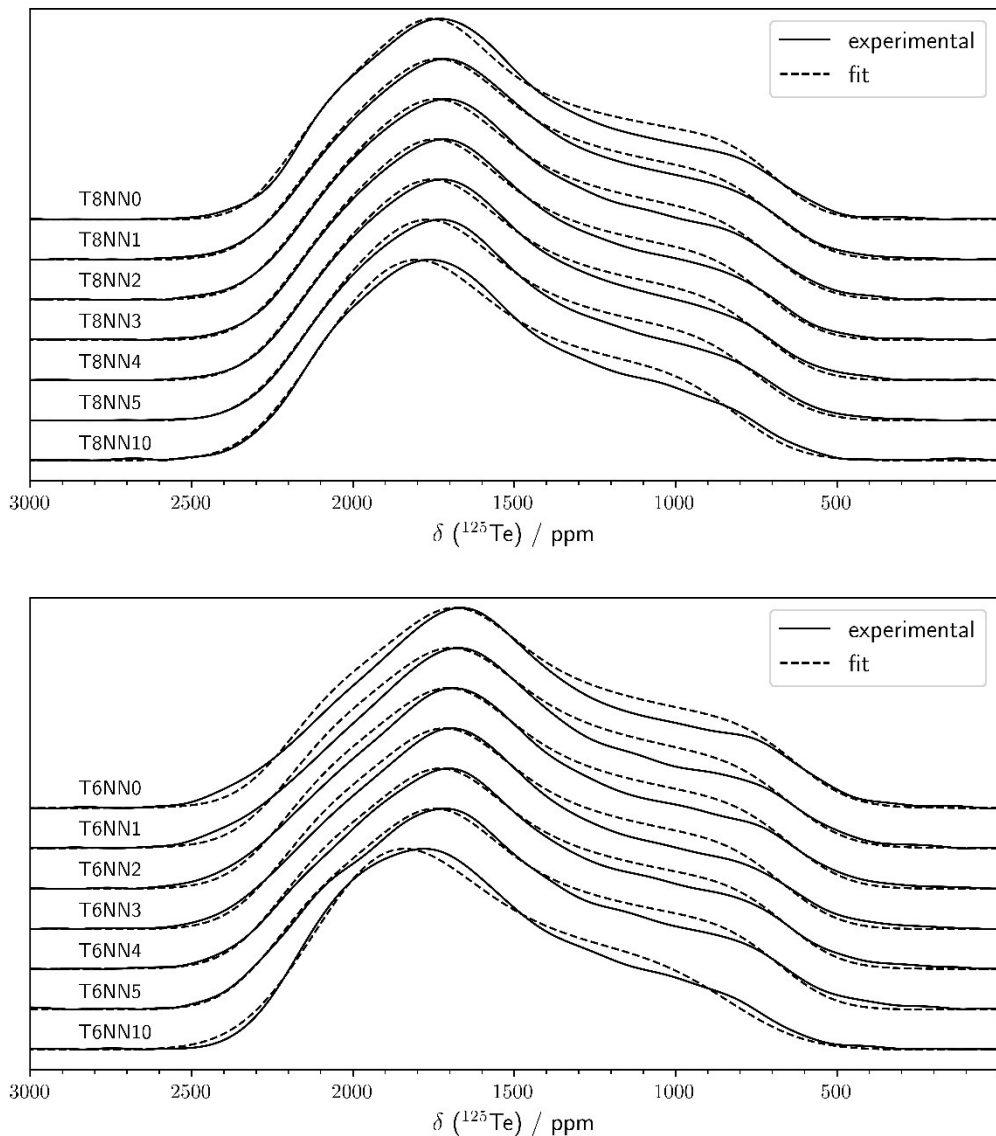


Figure S6. Static ^{125}Te NMR spectra of the samples under study. Dashed curves illustrate tentative fits assuming single Te-sites with the chemical shift tensor values listed in Table S4.

Table S4. Tentative ^{125}Te NMR lineshape fitting parameters for the glasses under study. Tensor elements are listed in the Haeberlen convention as well as principal axis values. The respective linebroadening parameter (lb) accounts for Gaussian type broadening of the resonance.

Sample	δ_{iso} / ppm	δ_{aniso} / ppm	η	δ_{11} / ppm	δ_{22} / ppm	δ_{33} / ppm	lb / kHz
T8NN0	1536	-854	0.52	2185	1740	682	27.2
T8NN1	1527	-848	0.54	2180	1722	679	30.6
T8NN2	1532	-839	0.53	2172	1729	693	30.9
T8NN3	1538	-834	0.54	2180	1729	704	30.3
T8NN4	1544	-828	0.53	2177	1739	716	30.9
T8NN5	1554	-820	0.51	2173	1755	734	32.1
T8NN10	1585	-790	0.48	2170	1790	795	33.4
T6NN0	1494	-878	0.59	2192	1674	616	29.4
T6NN1	1506	-870	0.59	2197	1684	636	30.7
T6NN2	1513	-880	0.59	2193	1693	633	31.1
T6NN3	1526	-871	0.59	2218	1704	655	31
T6NN4	1530	-884	0.58	2228	1716	646	29.5
T6NN5	1545	-879	0.57	2235	1734	666	30.7
T6NN10	1604	-795	0.36	2145	1858	809	40.1